



Published in final edited form as:

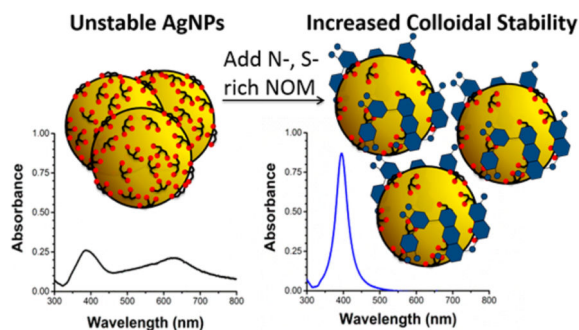
Environ Sci Technol. 2015 July 7; 49(13): 8078–8086. doi:10.1021/acs.est.5b01496.

Effects of Humic and Fulvic Acids on Silver Nanoparticle Stability, Dissolution, and Toxicity

Ian L. Gunsolus, Maral P. S. Mousavi, Kadir Hussein, Philippe Bühlmann*, and Christy L. Haynes*

Department of Chemistry, University of Minnesota, 207 Pleasant Street SE, Minneapolis, Minnesota 55455, United States

Abstract



The colloidal stability of silver nanoparticles (AgNPs) in natural aquatic environments influences their transport and environmental persistence, while their dissolution to Ag^+ influences their toxicity to organisms. Here, we characterize the colloidal stability, dissolution behavior, and toxicity of two industrially relevant classes of AgNPs (i.e., AgNPs stabilized by citrate or polyvinylpyrrolidone) after exposure to natural organic matter (NOM, i.e., Suwannee River Humic and Fulvic Acid Standards and Pony Lake Fulvic Acid Reference). We show that NOM interaction with the nanoparticle surface depends on (i) the NOM's chemical composition, where sulfur- and nitrogen-rich NOM more significantly increases colloidal stability, and (ii) the affinity of the capping agent for the AgNP surface, where nanoparticles with loosely bound capping agents are more effectively stabilized by NOM. Adsorption of NOM is shown to have little effect on AgNP dissolution under most experimental conditions, the exception being when the NOM is rich in sulfur and nitrogen. Similarly, the toxicity of AgNPs to a bacterial model (*Shewanella oneidensis* MR-1) decreases most significantly in the presence of sulfur- and nitrogen-rich NOM. Our data suggest that the rate of AgNP aggregation and dissolution in aquatic environments containing NOM will depend on the chemical composition of the NOM, and that the toxicity of AgNPs to aquatic microorganisms is controlled primarily by the extent of nanoparticle dissolution.

*Corresponding Authors: Phone: 612-624-1431; buhlmann@umn.edu. Phone: 612-626-1096; chaynes@umn.edu..

ASSOCIATED CONTENT

Supporting Information

Detailed methods, results of nanoparticle synthesis and characterization and related nanoparticle colloidal stability studies in presence of NOM, and explanation of ISE preparation and response. The Supporting Information is available free of charge on the ACS Publications website at DOI: 10.1021/acs.est.5b01496.

The authors declare no competing financial interest.

INTRODUCTION

Silver nanoparticles (AgNPs) are the most commonly used engineered nanomaterial in consumer products, serving primarily as antimicrobial agents (e.g., in fabrics and ointments).¹ Common product uses can result in leaching of AgNPs into water (e.g., through laundering or skin cleansing), which is expected to be the major route for AgNPs to enter the wastewater supply.^{2,3} Although a recent study demonstrated high removal efficiency of AgNPs in municipal wastewater treatment plants,⁴ AgNPs are also expected to enter natural environments through direct discharge from manufacturing and disposal of consumer and medical products that may circumvent wastewater treatment.^{3,5,6} Given the potential for AgNP entry into environments and their known toxicity to microorganisms,⁷ significant efforts are being made to identify the material and environmental parameters that control AgNP behavior and environmental impact.

AgNPs that enter natural aquatic environments encounter variable temperature, pH, light illumination, ionic strength, dissolved molecular oxygen concentration, and natural organic matter (NOM) concentration and composition. Each of these parameters has the potential to influence nanoparticle colloidal stability. These factors can also influence AgNP dissolution to give Ag⁺ (a process that depends on proton and molecular oxygen concentration),⁸ which is suggested to be the primary mode of AgNP toxicity to microorganisms.⁹⁻¹² Among the potential transformations of AgNPs entering natural aquatic environments, the least understood are those affected by NOM. A survey of the literature reveals variable effects of NOM on AgNP stability and dissolution, which appears to be caused by the high heterogeneity of NOM and the many AgNP models (in terms of size and surface chemistry) that have been employed.

Several studies have demonstrated that addition of purified, naturally extracted NOM at low parts-per-million concentrations decreases homoaggregation rates (i.e., increases colloidal stability) of AgNPs; this applies to both AgNPs electrostatically stabilized with a citrate capping agent and sterically stabilized with polyvinylpyrrolidone (PVP) as the capping agent.¹³⁻¹⁵ Similarly, increased stability of citrate-capped AgNPs in unpurified NOM suspensions was observed.¹⁶ A few notable exceptions to this trend were reported. For example, fulvic acids isolated from a reference site in a Norwegian lake, despite having elemental composition very similar to Suwannee River fulvic acid models that were shown to stabilize AgNPs, had no effect on AgNP stability at equivalent or higher NOM concentrations.¹⁷ Additionally, decreased colloidal stability of PVP-capped AgNPs following addition of cysteine (a simple model for protein-rich NOM) was observed in at least two studies.^{18,19} Our current understanding of NOM's impact on AgNP colloidal stability is complicated by results obtained using a wide range of nanomaterial-stabilizing agents and NOM types, and the general notion that NOM, despite its high chemical heterogeneity, can be considered as a class of molecules to have common patterns of interaction with AgNPs. Here, we identify the characteristics of NOM that most significantly impact the colloidal stability of AgNPs by employing in a single study a series of NOM types with variable chemical composition and nanoparticle capping agents.

The kinetics of AgNP dissolution, the equilibrium concentration of released Ag⁺, and complexation reactions of released Ag⁺ have been studied under variable solution conditions and with variable AgNP types. Discrepancies exist in the literature regarding the effect of NOM (either macromolecular or small molecule NOM models) on the extent of AgNP dissolution. Liu et al. observed decreased AgNP dissolution in the presence of thiol-containing species (e.g., cysteine and glutathione), which they attributed to a reduction in surface sites prone to oxidation.²⁰ In contrast, Gondikas et al. demonstrated increased dissolution of citrate- and PVP-capped AgNPs in the presence of cysteine.¹⁸ The latter authors attributed the discrepancy between the two studies to differences in sample preparation (specifically, the possibility for analyte retention and loss when using centrifugal filter units).¹⁸ Further studies employing other NOM models observed either significantly increased^{21,22} or decreased^{8,23} dissolution of AgNPs with increasing NOM concentration. We note that the majority of dissolution studies employ measurements of total Ag concentration, without discriminating between free Ag⁺ and Ag⁺-NOM complexes, though related work of ours demonstrated that Ag⁺ binding to NOM can in some cases mitigate Ag⁺ toxicity to bacteria.²⁴ In light of the important role of dissolved Ag⁺ (and Ag⁺-NOM complexes) to AgNP toxicity,^{9,24} and to address existing discrepancies in the literature, we used fluoros-phase Ag⁺ ion-selective electrodes (ISEs) for in situ detection of AgNP dissolution by monitoring the Ag⁺ concentration. Fluorophase Ag⁺ ISEs were previously shown to be powerful tools for dynamic monitoring of AgNP dissolution in complex media.²⁵

Several studies observed reduced toxicity of AgNPs toward a number of organismal models in the presence of NOM, but the mechanism of this effect remains unclear. Studies using bacterial models such as *Pseudomonas fluorescens*²⁶ and *Escherichia coli*²³ suggested the primary mechanism to be complexation of Ag⁺ with NOM, reducing its bioavailability or bactericidal activity. Other studies using *Pseudomonas fluorescens*²⁷ and the nematode *Caenorhabditis elegans*²⁸ suggested that NOM adsorption to AgNP surfaces (possibly decreasing total Ag⁺ release or modulating nanoparticle adsorption to or internalization by organisms) is the primary mechanism of toxicity mitigation. Through parallel measurements of Ag⁺ concentration and AgNP toxicity to a bacterium (*Shewanella oneidensis* MR-1), this study provides a more direct means to evaluate the mechanism of NOM mitigation of AgNP toxicity than was previously possible. It seeks to provide new insight on the molecular interaction of NOM with commercially relevant AgNPs stabilized with citrate or PVP. By employing a series of NOM models to represent major NOM classes, we arrive at fundamental and generalizable conclusions about AgNP-NOM interactions. Using in situ characterization, we avoid sample preparation errors that may have contributed to conflicting interpretations of prior results.

EXPERIMENTAL SECTION

Citrate-capped AgNPs were prepared using a reported method.¹⁶ PVP-capped AgNPs were prepared by incubating citrate-capped AgNPs with excess PVP-10 (average molecular weight 10 000 g/mol, Sigma-Aldrich), followed by purification. Ligand exchange was confirmed by zeta potential measurements, while particle size was determined using transmission electron microscopy. For details see the Supporting Information (SI).

Stock solutions of 10 g/L NOM (Suwannee River Humic Acid Standard II, Suwannee River Fulvic Acid Standard II or Pony Lake Fulvic Acid Reference, International Humic Substances Society, St. Paul, MN) were prepared in deionized water and mixed with aliquots of purified and concentrated AgNP suspensions to achieve a 600 mg/L NOM concentration. Nanoparticles were incubated with NOM in the dark without mixing for 18 h, followed by redispersion in 0.1 M ionic strength potassium phosphate buffer (pH 7.5, 5 mg Ag/L, 10 mg/L of NOM; acrylic cuvettes).

The colloidal stability of the resulting 3.0-mL AgNP samples was monitored over 2 days using UV–visible extinction spectroscopy and dark-field microscopy, and over 8 days using dynamic light scattering (DLS). Dissolution was monitored over 5 h in an identical buffer using fluorosphase Ag⁺ ISEs, prepared as described elsewhere²⁴ (see also the SI and Figure S4). Toxicity of AgNPs to *Shewanella oneidensis* MR-1 was evaluated using the LIVE/DEAD Cell Viability Assay (Invitrogen). For consistency, the cells were suspended in the buffer described above. For details see the SI.

RESULTS AND DISCUSSION

Impact of NOM and Nanoparticle Capping Agents on AgNP Colloidal Stability

AgNPs were prepared with either a citrate or PVP-10 capping agent to represent two major classes of industrially relevant AgNPs. TEM micrographs (SI Figure S1) reveal no appreciable change in AgNP morphology after exchanging citrate for PVP-10, demonstrating that nanoparticle surface functionalization can be varied independently from morphology. The average particle diameters of citrate- and PVP-capped AgNPs were calculated to be 12.1 ± 2.4 and 15.5 ± 4.1 nm, respectively, based on TEM analysis of 500 nanoparticles, indicating a minor, though statistically significant ($p < 0.001$), difference in nanoparticle size. Replacement of citrate by PVP-10 was probed by measuring the nanoparticle zeta potential. The latter decreased significantly with exchange to PVP-10, from -32.8 ± 2.2 to -13.6 ± 3.6 mV. These values are consistent with at least partial replacement of negatively charged citrate with neutral PVP-10 (SI Figure S1), and are in agreement with literature values for PVP-capped AgNPs prepared directly.^{18,29,30}

Initially, AgNPs were exposed to 10 mg/L NOM, chosen to fall within the concentration range of natural freshwaters (1–60 mg/L).³¹ Three types of NOM were used: Suwannee River fulvic acid (SRFA) and Suwannee River humic acid (SRHA) have similar elemental compositions³² (SI Table S1) and represent NOM fractions derived primarily from decomposition³³ of vegetation.³³ Pony Lake fulvic acid (PLFA) represents NOM rich in sites with high affinity for metallic silver and Ag⁺ (due to high sulfur and nitrogen content,³⁴ a subset of which has a high affinity for silver and Ag⁺;²⁴ SI Table S1). It is derived exclusively from microbial matter decomposition.³³ None of these had a detectable effect on AgNP colloidal stability when present at a concentration of 10 mg/L, as determined by UV–visible extinction spectroscopy (SI Figure S2). This technique was used to demonstrate changes in AgNP aggregation by monitoring the intensity and position of size-dependent extinction peaks due to the localized surface plasmon resonance effect. In subsequent experiments, AgNPs were exposed to a larger concentration of NOM (600 mg/L) prior to colloidal stability assessment to promote NOM interaction with the AgNP surface. This

simulates, on an accelerated time-scale, particle acquisition of adsorbed NOM, which is expected to take place over longer time periods in natural aquatic environments containing lower NOM concentrations. Following redispersion in a high ionic strength (0.1 M) buffer, the bulk NOM concentration during colloidal stability assessment was 10 mg/L. The ionic strength was chosen to ensure that the interaction of NOM with the AgNP surface was not purely electrostatic while remaining representative of natural aquatic systems.³⁵ Nanoparticle colloidal stability was monitored over 2 days again using UV–visible extinction spectroscopy (Figure 1).

The plasmon resonance of spherical metal nanoparticles causes light extinction features that are sensitive to interparticle interactions.³⁶ Such interactions shift the particle plasmon extinction peak to higher wavelengths.³⁶ In our study, a primary extinction peak attributable to the plasmon resonance frequency of nonagglomerated 12-nm-diameter AgNPs was observed at 391 and 394 nm for citrate- and PVP-capped AgNPs, respectively. The formation of variable-sized AgNP aggregates resulted in the appearance of a broader peak at longer wavelengths; larger aggregates produced broader and more red-shifted peaks. Similar observations of red-shifted UV–visible extinction spectra in response to AgNP aggregation were reported previously.³⁷ Nanoparticle aggregation was further characterized using dynamic light scattering (DLS) to track hydrodynamic particle diameter over time following dispersion in buffer (Figure 2). Extinction spectroscopy and DLS demonstrate that incubation with NOM stabilized citrate- and PVP-capped AgNPs against homoaggregation in a high ionic strength buffer (0.1 M) relative to their pristine (no-NOM) counterparts. The aggregation behavior of AgNPs is known to depend on surface characteristics, where surface coatings that promote steric repulsion are typically more effective at maintaining AgNP colloidal stability in high ionic strength environments than their counterparts promoting only electrostatic repulsion.^{38,39} However, surface-coating-dependent behavior of AgNPs in the presence of NOM has not been studied thoroughly. It was observed that citrate- and PVP-capped AgNPs aggregated similarly with increasing ionic strength after addition of cysteine, which was used as a low molecular weight model for NOM.¹⁸ However, higher molecular weight NOM, such as that used in our study, is expected to induce different effects, given its greater potential to increase steric repulsion between particles. In this study, the degree of AgNP stabilization conferred by NOM was dependent on both the NOM type and nanoparticle capping agent. Three primary effects were observed.

First, AgNPs exposed to high NOM concentrations had higher colloidal stability than pristine nanoparticles that were stabilized either electrostatically using citrate or sterically using PVP-10. Pristine citrate- and PVP-capped AgNPs aggregated immediately upon dispersion in phosphate buffer, as indicated by the low intensity of the primary extinction peak at 391 or 394 nm and the presence of a broad peak at longer wavelengths (Figure 1, left). The primary and secondary extinction peak intensities of citrate- and PVP-capped AgNPs decayed over time as the nanoparticles aggregated and fell out of suspension; particle dissolution (which was observed using ISEs and is discussed in more detail below) likely also contributed to decreasing intensity of the primary extinction peak. Rapid increases in the hydrodynamic particle diameters were observed over the first 3 h following dispersion (Figure 2), consistent with rapid formation of large aggregates. In contrast, citrate- and PVP-capped AgNPs that had been previously incubated with NOM showed a

higher intensity primary extinction peak at early time-points, indicating a larger population of stable 12-nm nanoparticles. Appearance of a broader, secondary extinction peak at red-shifted wavelengths was also slower, suggesting slower aggregate formation. In most cases, the average hydrodynamic particle diameter increased following dispersion in buffer, but increases were dramatically slower than for pristine nanoparticles. This result suggests that ligand-stabilized AgNPs that encounter high concentrations of NOM have significantly higher colloidal stability than their pristine counterparts. Whereas nanoparticle transport in natural aquatic environments depends not only on homoaggregation as evaluated here, but also on heteroaggregation and nanoparticle adsorption onto collector surfaces, our result suggests that AgNPs stabilized by NOM may be transported through aquatic environments more efficiently than their pristine counterparts, since homoaggregation and nanoparticle settling is reduced.

Second, the extent to which NOM increases AgNP colloidal stability depends on the affinity of the original organic capping agent for the nanoparticle surface. A fraction of PVP-capped AgNPs previously incubated with SRFA or SRHA aggregated immediately after dispersion in NOM-free buffer, resulting in a broad extinction peak between 500 and 750 nm (Figure 1, bottom). Equivalently prepared citrate-capped AgNPs aggregated more slowly and formed smaller aggregates, as indicated by slower growth of a narrower secondary extinction peak between 500 and 600 nm (Figure 1, top) and DLS measurement of hydrodynamic diameters (Figure 2). These results indicate that PVP-capped AgNPs are less effectively stabilized by NOM than citrate-capped AgNPs, which may be caused by the higher affinity of PVP than citrate for the AgNP surface. Citrate is generally thought to be weakly bound to the AgNP surface,³⁷ and citrate-capping of AgNPs is widely used in industry to provide stable precursors for other functionalization schemes due to the labile nature of this agent. At the high NOM concentrations employed in the current study, NOM may displace citrate from the nanoparticle surface. In contrast, PVP coordinates with the AgNP surface through van der Waals interactions and direct bonding interactions with the Ag *d*-band.^{40,41}

Computational studies showed that the latter occurs through bonding orbitals of the 2-pyrrolidone subunit, localized on the oxygen (~60%) and nitrogen (~25%).^{40,41} This is consistent with spectroscopic studies of PVP interaction with Ag, which suggested that direct bonding interactions occur through either only oxygen or a combination of oxygen and nitrogen.⁴²⁻⁴⁴ Because of direct bonding interactions with Ag, PVP is harder to displace than citrate, which may result in a greater barrier to NOM interaction with the nanoparticle surface. Alternatively, NOM might adsorb to either citrate or PVP on the AgNP surface, rather than displacing them. Under this assumption, our results suggest that more NOM binds to adsorbed citrate than to PVP since exposure to NOM induces a more significant increase in the colloidal stability of citrate- than PVP-capped AgNPs. However, at the pH of this system (pH 7.5), greater electrostatic repulsion exists between the negatively charged acidic residues of NOM and citrate (which carries three negative charges) than PVP (which is neutral). On the basis of our results, we conclude that AgNPs stabilized with easily displaceable organic capping agents will be more effectively stabilized by NOM.

Third, the extent to which NOM increases AgNP colloidal stability, regardless of the organic capping agent, depends on the concentration of sites with high affinity for metallic silver and

Ag⁺ (e.g., sulfur and nitrogen groups)⁴⁵ in the NOM. For both citrate- and PVP-capped AgNPs, the stabilizing power of NOM occurs in the order SRFA < SRHA << PLFA (Figures 1 and 2). Following dispersal of citrate-capped AgNPs exposed beforehand with SRFA or SRHA in NOM-free buffer (Figure 1, top middle), a broad, secondary extinction peak between 500 and 600 nm (due to variable size aggregates) appeared. This suggests that AgNPs previously incubated with SRFA and SRHA aggregate significantly, although less than AgNPs not treated with NOM. In contrast, no secondary extinction peak was observed following dispersion of AgNPs exposed before-hand with PLFA (top right), suggesting that no significant aggregation occurs in this case. In the case of PVP-capped AgNPs, PLFA is the only NOM type that eliminates immediate formation of a broad aggregate peak (Figure 1, bottom right). Because of the presence of both primary (12-nm-diameter) and variable-size nanoparticle aggregates in these samples, it was not possible to accurately determine the average hydrodynamic particle diameter by DLS using a single normal distribution model. Despite this limitation, the observed relative changes in estimated average hydrodynamic particle diameter were consistent with the extinction spectroscopy results. The estimated average hydrodynamic diameter of particles previously incubated with NOM increased most significantly over time when SRFA was used; this was true for both citrate- and PVP-capped AgNPs (Figure 2). In the case of citrate-capped AgNPs, the SRHA and PLFA incubation had indistinguishable effects on hydrodynamic particle diameter, but PLFA was a more effective stabilizing agent than SRHA in the case of PVP-capped AgNPs. Visual evidence for the relative stabilizing power of SRFA, SRHA, and PLFA is provided in SI Figure S3, which shows dark-field images and spatially resolved light scattering spectra of pristine and NOM-stabilized citrate-capped AgNPs 24 h after redispersion in buffer. These qualitative and semiquantitative results, respectively, confirm that citrate-capped AgNPs are increasingly stable when exposed to NOM in the order SRFA < SRHA << PLFA.

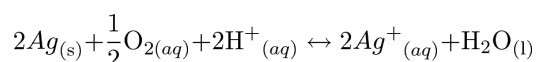
The three NOM types used in the current study were chosen because they have similar average molecular weights (between 1300 and 1400 Da)⁴⁶ but differ in sulfur and nitrogen content. Sulfur-containing species such as thiols have strong bonding interactions with metallic silver, and electron donating groups such as sulfur and nitrogen may act as Ag⁺-coordinating sites⁴⁷ when in the form, e.g., of thiols and amines. PLFA has approximately five to six times more total sulfur than either SRHA or SRFA (SI Table S1),³⁴ with approximately twice the fractional exocyclic sulfur content (e.g., thiol) of SRHA and SRFA.⁴⁸ This results in an approximately 11 times higher thiol content of PLFA over SRHA and SRFA. Given the ability of thiols to form stable complexes with metals including silver⁴⁹ and also with Ag⁺ (which was shown to adsorb to the nanoparticle surface⁸), the observed NOM ranking (PLFA >> SRHA > SRFA) may be partly attributable to their relative thiol contents. PLFA also has five to ten times more total nitrogen than SRHA or SRFA.³⁴ This higher nitrogen content, present to a significant extent in the form of amides, amines, and heterocyclic nitrogens,⁵⁰ may also contribute to the greater stabilizing effect of PLFA. This explanation is also consistent with the latter ranking (SRHA > SRFA), since SRHA has an approximately two times higher nitrogen content than SRFA but is otherwise chemically similar (SI Table S1). Given the lower oxygen content of PLFA than SRFA or SRHA (SI Table S1), the relative NOM ranking observed here suggests that electron donating groups containing oxygen (e.g., carboxylic acids and phenols) have less influence

on AgNP colloidal stability than electron donating groups like sulfur and nitrogen. The relative NOM ranking observed here is consistent with that observed in a study considering Ag⁺ only.²⁴

We point out that while SRFA and SRHA have similar average molecular weights (1400 Da for SRHA, 1360 Da for SRFA),⁵¹ their molecular weight distributions are different, with a larger fraction of higher molecular weight NOM in SRHA than SRFA.⁵² A previous study of citrate-capped gold nanoparticle stability with NOM suggested that high molecular weight fractions have much larger effects on nanoparticle stability than low molecular weight fractions separated from the same NOM source.⁵³ Therefore, we suggest that preferential interaction of high molecular weight NOM fractions with AgNPs may also contribute to the increased colloidal stability of SRHA- over SRFA-stabilized AgNPs. PLFA has a molecular weight distribution similar to that of SRFA⁵⁴ yet has a much greater effect on AgNP colloidal stability than SRFA or SRHA, as described above. Consequently, we suggest that sulfur and nitrogen content (i.e., sites with high affinity for metallic silver and Ag⁺) plays a significant role in determining NOM's interaction with AgNPs in addition to molecular weight.

Impact of NOM on AgNP Dissolution

The oxidative dissolution of AgNPs in natural aquatic environments is of interest due to the potential toxicity of released Ag⁺ to microorganisms. In the absence of other oxidizing or reducing agents, AgNP dissolution proceeds with the following stoichiometry:⁸



The literature presents sometimes conflicting results regarding the effect of NOM on AgNP dissolution. For example, adsorption of thiol-containing species, such as cysteine, was shown to either inhibit^{20,29} or increase¹⁸ AgNP dissolution. Such discrepancies may result from errors introduced during separation of AgNPs from dissolved Ag⁺ (e.g., from retention of Ag⁺ on centrifugal filters).¹⁸ A separation step is necessary when monitoring AgNP dissolution by spectroscopic or spectrometric techniques, as these techniques cannot discriminate between Ag⁺ and AgNPs. In the current study, we employ fluorine-phase Ag⁺ ISEs to monitor AgNP dissolution in situ, thereby eliminating the need for sample preparation and reducing potential sampling errors.²⁵

We investigated the effect of NOM composition on the dissolution of 12-nm-diameter citrate-capped AgNPs under an environmentally relevant condition (pH 7.5 phosphate buffer, as used above, and 10 mg/L NOM concentration in the bulk solution). Citrate-capped AgNPs that had been previously incubated with a high concentration of NOM (600 mg/L) were added to the pH buffer, yielding a silver concentration of 5 mg/L and a bulk NOM concentration of 10 mg/L. (Experiments were also conducted using AgNPs that had not been previously incubated with a high concentration of NOM, but the presence of 10 mg/L NOM in solution had no statistically significant effect on nanoparticle dissolution; SI Figure S5.) Changes in the concentration of Ag⁺ were then monitored by measuring the electromotive

force, emf, of the fluoruous-phase Ag^+ ISE with respect to a reference electrode placed into the same solution. At a constant temperature, the emf of fluoruous-phase Ag^+ ISEs increases linearly with the logarithm of the Ag^+ activity. For example, at 20 °C a 10-fold increase in the activity of Ag^+ results in a 58.2 mV increase in emf.⁵⁵ The theoretical response and calibration of Ag^+ fluoruous-phase ISEs are explained in the SI and illustrated in Figure S4.

Figure 3a shows the results of ISE monitoring of nanoparticle dissolution. A sudden increase in the emf after addition of the AgNPs is caused by NP dissolution to give Ag^+ ions. The emf becomes stable 1 h after AgNP addition, indicating that the concentration of Ag^+ in solution has reached a steady state. The gradual increase in emf represents an increase in free silver concentration and not a slow response time of the electrode, as shown by the nearly instantaneous (less than 1 s) response of the ISE to changes in Ag^+ concentration caused by hydrogen peroxide and NaCl additions. While hydrogen peroxide oxidizes AgNPs and increases the Ag^+ concentration in solution, chloride precipitates Ag^+ , reducing the concentration of Ag^+ in solution. Both effects are detected quickly by the ISE, illustrating the advantage of this sensor for dynamic in situ detection.

The effect of NOM with variable chemical composition on AgNP dissolution is presented in Figure 3b. SRHA- and SRFA-stabilized citrate-capped AgNPs showed Ag^+ release profiles over time equivalent to pristine nanoparticles (without NOM). Given the significantly increased colloidal stability of SRHA- and SRFA-stabilized AgNPs over pristine AgNPs, their similar dissolution profiles suggest that dissolution is relatively insensitive to nanoparticle aggregation state. This is consistent with previous reports, which suggested that AgNP aggregation only minimally decreases the surface area available for interaction with molecular oxygen.^{8,56} In contrast to SRHA- and SRFA-stabilized AgNPs, PLFA-stabilized citrate-capped AgNPs released over 5 h approximately one-half the Ag^+ content of pristine nanoparticles. This result most likely reflects the high sulfur and nitrogen content of PLFA, as described above. Sulfur-containing functionalities, specifically thiol groups, have high affinities for silver surfaces, while thiolates and amines can form complexes with Ag^+ . NOM bound to the AgNP surface (e.g., through interaction of thiol-containing species with metallic silver or thiolates and amines with surface-adsorbed Ag^+) may exclude molecular oxygen from active sites and thereby limit oxidative dissolution, as previously suggested in the case of thiols.²⁰ Our results demonstrate that even when AgNPs are exposed to a very high NOM concentration (600 mg/L), there is a minimal effect on Ag^+ release except when the NOM has a high concentration of strongly Ag-coordinating sites. Perhaps more surprising is the observation that prior incubation with SRHA or SRFA, which significantly stabilizes AgNPs against homoaggregation (as shown in our colloidal stability experiments), had no effect on the rate and total amount of Ag^+ released.

We also compared the dissolution of citrate-capped and PVP-capped AgNPs. Exchanging a fraction of citrate for PVP-10 induced a significant decrease (~40%) in Ag^+ release over 5 h. Previous reports suggested that PVP may have high affinity for not only Ag surfaces but also Ag^+ ,⁵⁷ an effect that could trap Ag^+ at the particle surface and buffer its release into solution.²⁰ To directly test this hypothesis, we used Ag^+ ISEs to monitor the concentration of free Ag^+ in solution after addition of PVP. We observed no detectable changes in free Ag^+ concentration after addition of up to 50 mg/L PVP (SI Figure S6), indicating that PVP has

low affinity for Ag^+ and is unlikely to trap Ag^+ ions at the AgNP surface. An alternative mechanism to explain the observed PVP-induced decrease in AgNP dissolution is surface passivation. Although it is beyond the scope of this work to directly assess the validity of this mechanism, we note Grubbs' suggestion that some polymer ligands can control access of molecular oxygen to the nanoparticle surface,⁵⁸ which would decrease the oxidative dissolution rate of AgNPs. We note that the total dissolved Ag^+ concentration in our experiments corresponds to approximately 1–2% (depending on the capping agent) of the total silver content present in the original AgNP suspension, consistent with previous dissolution studies using larger (39 nm) PVP-capped AgNPs.²⁹

Impact of NOM on AgNP Toxicity to Bacteria

Previous work suggested that AgNP toxicity to bacteria can be fully attributed to the bioavailable Ag^+ concentration resulting from nanoparticle dissolution.⁹ A recent report suggested that while AgNPs and Ag^+ may have similar effects on bacterial survival, they have distinct mechanisms of antibacterial activity.⁵⁹ Although questions remain regarding the relationship between AgNP dissolution and toxicity to bacteria, understanding AgNP dissolution in environmental matrices remains a critical step toward understanding the implications of their release into natural aquatic environments. To this end, a few studies assessed the role of Ag^+ -complexing agents, such as NOM, on resultant AgNP toxicity to bacteria. Fabrega et al. demonstrated reduced toxicity of citrate-capped AgNPs to *Pseudomonas fluorescens* with addition of 10 mg/L SRHA at pH 9.0, but no reduction of Ag^+ toxicity at an equivalent concentration.²⁷ They hypothesized that reduction of AgNP toxicity caused by SRHA may be due to its role as a physical barrier to cell–NP contact or as a ROS-scavenger (antioxidant), while its lack of effect on Ag^+ toxicity may be due to insignificant binding with Ag^+ or continued bioavailability of Ag^+ in the complexed form. Zhang et al. demonstrated reduced bacterial disinfection performance of PVP-capped AgNPs following addition of 5 mg/L SRHA, an effect that they attributed to an observed reduction in Ag^+ release under these conditions.²³ As these examples demonstrate, disagreements persist regarding the effect of NOM on AgNP dissolution and toxicity to bacteria, perhaps in part due to the use of indirect measurements of AgNP dissolution and lack of Ag speciation information. Here, we coupled direct measurements of Ag^+ dissolution from AgNPs in the presence of NOM (described above) with an assessment of AgNP toxicity to *Shewanella oneidensis* MR-1 to provide novel insight into the mechanism of NOM's effect on AgNP bactericidal efficacy.

In these toxicity experiments, as in previously described nanoparticle colloidal stability experiments, AgNPs were initially exposed to a high concentration of NOM, and were then redispersed in NOM-free buffer. *Shewanella oneidensis* MR-1 was mixed with NOM-treated citrate- or PVP-capped AgNPs, and cellular membrane integrity was evaluated as a function of NOM type. Nanoparticle-induced membrane damage, a known mechanism of AgNP bactericidal activity,^{11,60} was observed by monitoring the relative fluorescence emission intensities of two nucleic acid probes, one of which is cell membrane-permeable, thus labeling all cells, and one which is cell membrane-impermeable, thus labeling only membrane-compromised cells. The relative fraction of membrane-compromised cells in a

sample was then determined by calculating the ratio of fluorescence emission intensity of these probes normalized to a sample receiving no nanoparticle treatment.

Our results (Figure 3c) demonstrate that the bactericidal efficacy of citrate-capped AgNPs was reduced after exposure to PLFA, while SRFA and SRHA had no effect. This is consistent with the results of our ISE dissolution studies, which indicated that PLFA was the only NOM type to significantly reduce Ag⁺ release from AgNPs (Figure 3b). The relative impact of the NOM types used here on AgNP dissolution is also consistent with the results of our related study in which ISEs were used to measure Ag⁺ binding to NOM in the absence of AgNPs.²⁴ Addition of PLFA to a Ag⁺ solution significantly decreased the free Ag⁺ concentration, indicating binding of NOM to Ag⁺, while SRHA and SRFA induced smaller decreases. In the present study, PVP-capped AgNPs were also observed to be less toxic than citrate-capped AgNPs, consistent with their significantly lower release of Ag⁺ (Figure 3b). Complexation of Ag⁺ with NOM on the nanoparticle surface or in the bulk may decrease its bulk concentration and lower the bactericidal efficacy of the nanoparticle. Passivation of the nanoparticle surface by adsorbed or covalently bound NOM may also suppress Ag⁺ release in a way analogous to that described above for PVP. Although direct evaluation of these proposed mechanisms is beyond the scope of this work, we note Liu et al.'s suggestion that both Ag⁺ complexation with surface capping agents and AgNP surface passivation by ligands with high Ag affinity are chemical approaches to control Ag⁺ release from AgNPs.²⁰ Some studies suggested that NOM may reduce AgNP toxicity indirectly, that is, by influencing processes other than nanoparticle dissolution (e.g., AgNP interaction with the bacterial cell surface or scavenging of reactive oxygen species).²⁷ Although our results do not exclude this possibility, they suggest that AgNP toxicity to bacteria is highly dependent on nanoparticle dissolution, a process that is in turn dependent on the chemical composition of the nanoparticle capping agent and, if present, NOM.

The results of our AgNP colloidal stability, dissolution, and toxicity studies suggest that NOM with high affinity for Ag (i.e., NOM rich in some sulfur and nitrogen compounds) will induce the greatest increase in AgNP colloidal stability, the greatest decrease in nanoparticle release of Ag⁺, and the greatest decrease in AgNP bactericidal efficacy. NOM with lower affinity for Ag (i.e., NOM lower in reduced sulfur and nitrogen) will increase AgNP colloidal stability but have limited impact on nanoparticle release of Ag⁺ or bactericidal efficacy, potentially increasing the persistence and impact of AgNPs in natural aquatic environments. The magnitude of this effect is expected to depend on the relative concentrations of NOM in the bulk solution (where higher concentrations lead to greater complexation of NOM with Ag⁺ and may in some cases reduce AgNP bactericidal efficacy),²⁴ and on the particle surface (where higher concentrations lead to greater colloidal stability but, in some cases, have no impact on Ag⁺ release relative to less colloidal stable AgNPs). In addition, our results indicate that exposure to NOM improves the colloidal stability of AgNPs by delaying the onset of aggregation rather than by eliminating it completely. We show that NOM can reduce the rate of AgNP aggregation over 1–8 days, but additional studies are needed to understand the longer-term aggregation behavior of AgNPs exposed to NOM. The present results and those of our study considering Ag⁺ only²⁴ suggest that the effect of NOM on the bactericidal efficacies of Ag⁺ and AgNPs are not easily predicted by either the magnitude of NOM–Ag⁺ complexation or the extent of NOM

association with the AgNP surface. Therefore, the consequences of AgNP release into natural aquatic ecosystems containing NOM must be evaluated in an environment-specific context.

Supplementary Material

Refer to Web version on PubMed Central for supplementary material.

ACKNOWLEDGMENTS

This work was supported by a UMN Doctoral Dissertation Fellowship to M.P.S.M., UMN Biotechnology Institute Training Grant and Torske Klubben Fellowship to I.L.G., Heisig/Gleysteen Fellowship to K.H., and NSF Award CHE-1152931. Parts of this work were performed at the UMN Characterization Facility, which receives partial support from the MRSEC NSF program. Thanks to Katie Hurley and Samuel Egger for acquiring TEM images.

REFERENCES

- (1). Archived: The Project on Emerging Nanotechnologies at the Woodrow Wilson International Center for Scholars. 2011. <http://www.nanotechproject.org/inventories/silver/>
- (2). Kaegi R, Voegelin A, Sinnet B, Zuleeg S, Hagedorfer H, Burkhardt M, Siegrist H. Behavior of Metallic Silver Nanoparticles in a Pilot Wastewater Treatment Plant. *Environ. Sci. Technol.* 2011; 45:3902–3908. [PubMed: 21466186]
- (3). Benn TM, Westerhoff P. Nanoparticle Silver Released into Water from Commercially Available Sock Fabrics. *Environ. Sci. Technol.* 2008; 42:4133–4139. [PubMed: 18589977]
- (4). Li L, Hartmann G, Döblinger M, Schuster M. Quantification of Nanoscale Silver Particles Removal and Release from Municipal Wastewater Treatment Plants in Germany. *Environ. Sci. Technol.* 2013; 47:7317–7323. [PubMed: 23750458]
- (5). Marambio-Jones C, Hoek EMV. A Review of the Antibacterial Effects of Silver Nanomaterials and Potential Implications for Human Health and the Environment. *J. Nanopart. Res.* 2010; 12:1531–1551.
- (6). Mueller NC, Nowack B. Exposure Modeling of Engineered Nanoparticles in the Environment. *Environ. Sci. Technol.* 2008; 42:4447–4453. [PubMed: 18605569]
- (7). Rai M, Yadav A, Gade A. Silver Nanoparticles as a New Generation of Antimicrobials. *Biotechnol. Adv.* 2009; 27:76–83. [PubMed: 18854209]
- (8). Liu J, Hurt RH. Ion Release Kinetics and Particle Persistence in Aqueous Nano-Silver Colloids. *Environ. Sci. Technol.* 2010; 44:2169–2175. [PubMed: 20175529]
- (9). Xiu Z, Zhang Q, Puppala HL, Colvin VL, Alvarez PJ. Negligible Particle-Specific Antibacterial Activity of Silver Nanoparticles. *Nano Lett.* 2012; 12:4271–4275. [PubMed: 22765771]
- (10). Xiu Z-M, Ma J, Alvarez PJJ. Differential Effect of Common Ligands and Molecular Oxygen on Antimicrobial Activity of Silver Nanoparticles versus Silver Ions. *Environ. Sci. Technol.* 2011; 45:9003–9008. [PubMed: 21950450]
- (11). Hwang ET, Lee JH, Chae YJ, Kim YS, Kim BC, Sang B-I, Gu MB. Analysis of the Toxic Mode of Action of Silver Nanoparticles Using Stress-Specific Bioluminescent Bacteria. *Small.* 2008; 4:746–750. [PubMed: 18528852]
- (12). Jung WK, Koo HC, Kim KW, Shin S, Kim SH, Park YH. Antibacterial Activity and Mechanism of Action of the Silver Ion in *Staphylococcus aureus* and *Escherichia coli*. *Appl. Environ. Microbiol.* 2008; 74:2171–2178. [PubMed: 18245232]
- (13). Huynh KA, Chen KL. Aggregation Kinetics of Citrate and Polyvinylpyrrolidone Coated Silver Nanoparticles in Monovalent and Divalent Electrolyte Solutions. *Environ. Sci. Technol.* 2011; 45:5564–5571. [PubMed: 21630686]
- (14). Yu S, Yin Y, Chao J, Shen M, Liu J. Highly Dynamic PVP-Coated Silver Nanoparticles in Aquatic Environments: Chemical and Morphology Change Induced by Oxidation of Ag⁰ and Reduction of Ag⁺. *Environ. Sci. Technol.* 2013; 48:403–411. [PubMed: 24328224]

- (15). Angel BM, Batley GE, Jarolimek CV, Rogers NJ. The Impact of Size on the Fate and Toxicity of Nanoparticulate Silver in Aquatic Systems. *Chemosphere*. 2013; 93:359–365. [PubMed: 23732009]
- (16). Chinnapongse SL, MacCuspie RI, Hackley VA. Persistence of Singly Dispersed Silver Nanoparticles in Natural Freshwaters, Synthetic Seawater, and Simulated Estuarine Waters. *Sci. Total Environ*. 2011; 409:2443–2450. [PubMed: 21481439]
- (17). Li X, Lenhart JJ, Walker HW. Dissolution-Accompanied Aggregation Kinetics of Silver Nanoparticles. *Langmuir*. 2010; 26:16690–16698. [PubMed: 20879768]
- (18). Gondikas AP, Morris A, Reinsch BC, Marinakos SM, Lowry GV, Hsu-Kim H. Cysteine-Induced Modifications of Zero-Valent Silver Nanomaterials: Implications for Particle Surface Chemistry, Aggregation, Dissolution, and Silver Speciation. *Environ. Sci. Technol*. 2012; 46:7037–7045. [PubMed: 22448900]
- (19). Yang X, Lin S, Wiesner MR. Influence of Natural Organic Matter on Transport and Retention of Polymer Coated Silver Nanoparticles in Porous Media. *J. Hazard. Mater*. 2014; 264:161–168. [PubMed: 24295767]
- (20). Liu J, Sonshine DA, Shervani S, Hurt RH. Controlled Release of Biologically Active Silver from Nanosilver Surfaces. *ACS Nano*. 2010; 4:6903–6913. [PubMed: 20968290]
- (21). Pokhrel LR, Dubey B, Scheuerman PR. Natural Water Chemistry (dissolved Organic Carbon, pH, and Hardness) Modulates Colloidal Stability, Dissolution, and Antimicrobial Activity of Citrate Functionalized Silver Nanoparticles. *Environ. Sci. Nano*. 2014; 1:45.
- (22). Pokhrel LR, Dubey B, Scheuerman PR. Impacts of Select Organic Ligands on the Colloidal Stability, Dissolution Dynamics, and Toxicity of Silver Nanoparticles. *Environ. Sci. Technol*. 2013; 47:12877–12885. [PubMed: 24144348]
- (23). Zhang H, Smith JA, Oyanedel-Craver V. The Effect of Natural Water Conditions on the Anti-Bacterial Performance and Stability of Silver Nanoparticles Capped with Different Polymers. *Water Res*. 2012; 46:691–699. [PubMed: 22169660]
- (24). Mousavi, MPS.; Gunsolus, IL.; Perez De Jesus, CE.; Lancaster, M.; Hussein, K.; Haynes, CL.; Buhlmann, P. Dynamic Silver Speciation as Studied with Fluorous-phase Ion-selective Electrodes: Effect of Natural Organic Matter on the Toxicity and Speciation of Silver. submitted
- (25). Maurer-Jones MA, Mousavi MPS, Chem LD, Buhlmann P, Haynes CL. Characterization of Silver Ion Dissolution from Silver Nanoparticles Using Fluorous-Phase Ion-Selective Electrodes and Assessment of Resultant Toxicity to *Shewanella oneidensis*. *Chem. Sci*. 2013; 4:2564–2572.
- (26). Wirth SM, Lowry GV, Tilton RD. Natural Organic Matter Alters Biofilm Tolerance to Silver Nanoparticles and Dissolved Silver. *Environ. Sci. Technol*. 2012; 46:12687–12696. [PubMed: 23110472]
- (27). Fabrega J, Fawcett SR, Renshaw JC, Lead JR. Silver Nanoparticle Impact on Bacterial Growth: Effect of pH, Concentration, and Organic Matter. *Environ. Sci. Technol*. 2009; 43:7285–7290. [PubMed: 19848135]
- (28). Yang X, Jiang C, Hsu-Kim H, Badireddy AR, Dykstra M, Wiesner M, Hinton DE, Meyer JN. Silver Nanoparticle Behavior, Uptake, and Toxicity in *Caenorhabditis elegans*: Effects of Natural Organic Matter. *Environ. Sci. Technol*. 2014; 48:3486–3495. [PubMed: 24568198]
- (29). Levard C, Reinsch BC, Michel FM, Oumahi C, Lowry GV, Brown GE. Sulfidation Processes of PVP-Coated Silver Nanoparticles in Aqueous Solution: Impact on Dissolution Rate. *Environ. Sci. Technol*. 2011; 45:5260–5266. [PubMed: 21598969]
- (30). Kittler S, Greulich C, Diendorf J, Köller M, Epple M. Toxicity of Silver Nanoparticles Increases during Storage Because of Slow Dissolution under Release of Silver Ions. *Chem. Mater*. 2010; 22:4548–4554.
- (31). Robertson AI, Bunn SE, Boon PI, Walker KF. Sources, Sinks and Transformations of Organic Carbon in Australian Floodplain Rivers. *Mar. Freshwater Res*. 1999; 50:813–829.
- (32). Acidic Functional Groups of IHSS Samples. [accessed June 26, 2014] 2013. <http://www.humicsubstances.org/acidity.html>
- (33). Source Materials for IHSS Samples. [accessed June 26, 2014] 2013. <http://www.humicsubstances.org/sources.html>

- (34). Elemental Compositions and Stable Isotopic Ratios of IHSS Samples. [accessed June 26, 2014] 2013. <http://www.humicsubstances.org/elements.html>
- (35). Millero FJ. The Physical Chemistry of Natural Waters. *Pure Appl. Chem.* 1985; 57:1015–1024.
- (36). Zeman EJ, Schatz GC. An Accurate Electromagnetic Theory Study of Surface Enhancement Factors for Silver, Gold, Copper, Lithium, Sodium, Aluminum, Gallium, Indium, Zinc, and Cadmium. *J. Phys. Chem.* 1987; 91:634–643.
- (37). Tejamaya M, Römer I, Merrifield RC, Lead JR. Stability of Citrate, PVP, and PEG Coated Silver Nanoparticles in Ecotoxicology Media. *Environ. Sci. Technol.* 2012; 46:7011–7017. [PubMed: 22432856]
- (38). Li Y, Zhang W, Niu J, Chen Y. Surface-Coating-Dependent Dissolution, Aggregation, and Reactive Oxygen Species (ROS) Generation of Silver Nanoparticles under Different Irradiation Conditions. *Environ. Sci. Technol.* 2013; 47:10293–10301. [PubMed: 23952964]
- (39). Badawy AME, Luxton TP, Silva RG, Sheckel KG, Suidan MT, Tolaymat TM. Impact of Environmental Conditions (pH, Ionic Strength, and Electrolyte Type) on the Surface Charge and Aggregation of Silver Nanoparticles Suspensions. *Environ. Sci. Technol.* 2010; 44:1260–1266. [PubMed: 20099802]
- (40). Saidi WA, Feng H, Fichthorn KA. Binding of Polyvinylpyrrolidone to Ag Surfaces: Insight into a Structure-Directing Agent from Dispersion-Corrected Density Functional Theory. *J. Phys. Chem. C.* 2012; 117:1163–1171.
- (41). Al-Saidi WA, Feng H, Fichthorn KA. Adsorption of Polyvinylpyrrolidone on Ag Surfaces: Insight into a Structure-Directing Agent. *Nano Lett.* 2011; 12:997–1001. [PubMed: 22206357]
- (42). Huang HH, Ni XP, Loy GL, Chew CH, Tan KL, Loh FC, Deng JF, Xu GQ. Photochemical Formation of Silver Nanoparticles in Poly(*N*-Vinylpyrrolidone). *Langmuir.* 1996; 12:909–912.
- (43). Wang H, Qiao X, Chen J, Wang X, Ding S. Mechanisms of PVP in the Preparation of Silver Nanoparticles. *Mater. Chem. Phys.* 2005; 94:449–453.
- (44). Zhang Z, Zhao B, Hu L. PVP Protective Mechanism of Ultrafine Silver Powder Synthesized by Chemical Reduction Processes. *J. Solid State Chem.* 1996; 121:105–110.
- (45). Sikora FJ, Stevenson FJ. Silver Complexation by Humic Substances: Conditional Stability Constants and Nature of Reactive Sites. *Geoderma.* 1988; 42:353–363.
- (46). Deonaraine A, Lau BLT, Aiken GR, Ryan JN, Hsu-Kim H. Effects of Humic Substances on Precipitation and Aggregation of Zinc Sulfide Nanoparticles. *Environ. Sci. Technol.* 2011; 45:3217–3223. [PubMed: 21291228]
- (47). Gordon O, Slenters TV, Brunetto PS, Villaruz AE, Sturdevant DE, Otto M, Landmann R, Fromm KM. Silver Coordination Polymers for Prevention of Implant Infection: Thiol Interaction, Impact on Respiratory Chain Enzymes, and Hydroxyl Radical Induction. *Antimicrob. Agents Chemother.* 2010; 54:4208–4218. [PubMed: 20660682]
- (48). Manceau A, Nagy KL. Quantitative Analysis of Sulfur Functional Groups in Natural Organic Matter by XANES Spectroscopy. *Geochim. Cosmochim. Acta.* 2012; 99:206–223.
- (49). Vos, JG.; Forster, RJ.; Keyes, TE. *Interfacial Supramolecular Assemblies.* Wiley; New York: 2003. p. 90-91.
- (50). Thorn KA, Cox LG. N-15 NMR Spectra of Naturally Abundant Nitrogen in Soil and Aquatic Natural Organic Matter Samples of the International Humic Substances Society. *Org. Geochem.* 2009; 40:484–499.
- (51). Waples JS, Nagy KL, Aiken GR, Ryan JN. Dissolution of Cinnabar (HgS) in the Presence of Natural Organic Matter. *Geochim. Cosmochim. Acta.* 2005; 69:1575–1588.
- (52). Hyung H, Kim J-H. Natural Organic Matter (NOM) Adsorption to Multi-Walled Carbon Nanotubes: Effect of NOM Characteristics and Water Quality Parameters. *Environ. Sci. Technol.* 2008; 42:4416–4421. [PubMed: 18605564]
- (53). Louie SM, Tilton RD, Lowry GV. Effects of Molecular Weight Distribution and Chemical Properties of Natural Organic Matter on Gold Nanoparticle Aggregation. *Environ. Sci. Technol.* 2013; 47:4245–4254. [PubMed: 23550560]
- (54). Duarte RMBO, Barros AC, Duarte AC. Resolving the Chemical Heterogeneity of Natural Organic Matter: New Insights from Comprehensive Two-Dimensional Liquid Chromatography. *J. Chromatogr.* 2012; 1249:138–146.

- (55). Buhlmann, P.; Chen, LD. *Supramolecular Chemistry: From Molecules to Nanomaterials*. Wiley; New York: 2012. Ion-Selective Electrodes With Ionophore-Doped Sensing Membranes; p. 2539-2579.
- (56). Zhang W, Yao Y, Sullivan N, Chen Y. Modeling the Primary Size Effects of Citrate-Coated Silver Nanoparticles on Their Ion Release Kinetics. *Environ. Sci. Technol.* 2011; 45:4422–4428. [PubMed: 21513312]
- (57). Chen D, Qiao X, Qiu X, Chen J. Synthesis and Electrical Properties of Uniform Silver Nanoparticles for Electronic Applications. *J. Mater. Sci.* 2009; 44:1076–1081.
- (58). Grubbs RB. Roles of Polymer Ligands in Nanoparticle Stabilization. *Polym. Rev.* 2007; 47:197–215.
- (59). Ivask A, ElBadawy A, Kaweeteerawat C, Boren D, Fischer H, Ji Z, Chang CH, Liu R, Tolaymat T, Telesca D, et al. Toxicity Mechanisms in *Escherichia coli* Vary for Silver Nanoparticles and Differ from Ionic Silver. *ACS Nano.* 2013; 8:374–386. [PubMed: 24341736]
- (60). Sondi I, Salopek-Sondi B. Silver Nanoparticles as Antimicrobial Agent: A Case Study on *E. coli* as a Model for Gram-Negative Bacteria. *J. Colloid Interface Sci.* 2004; 275:177–182. [PubMed: 15158396]

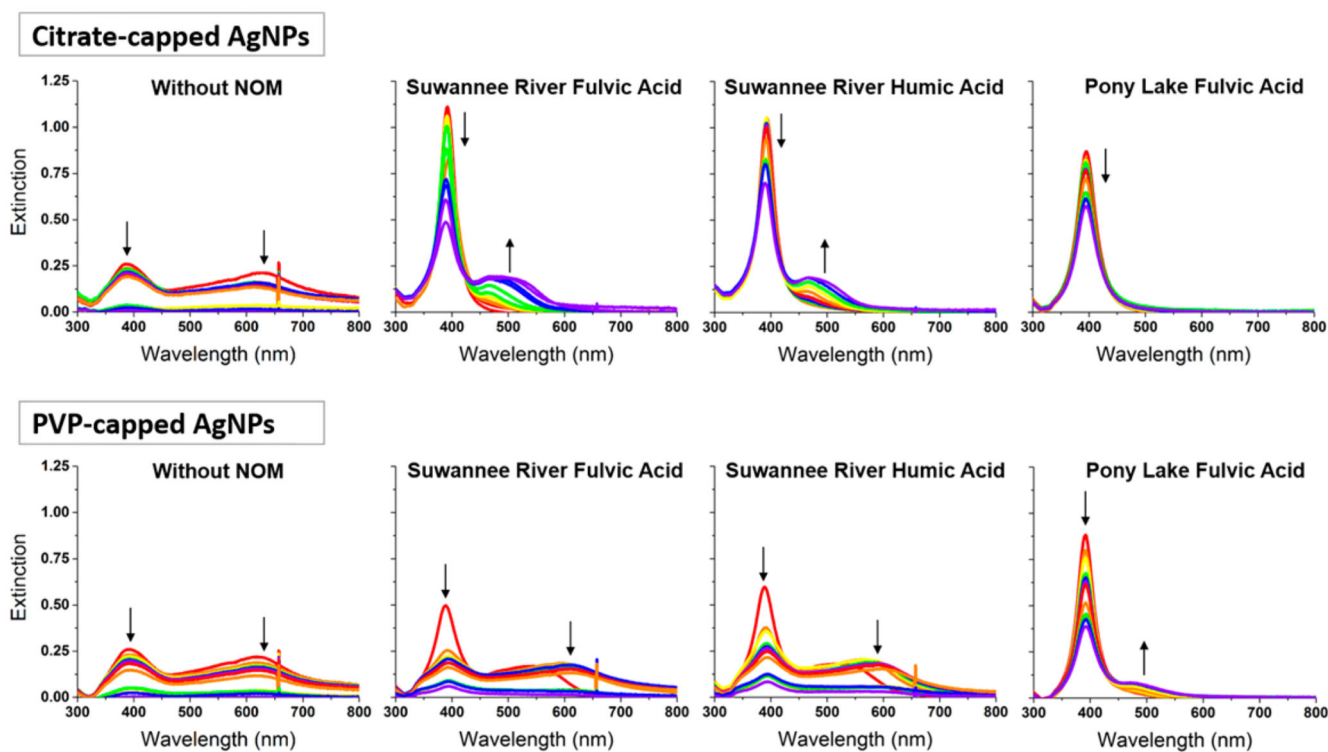


Figure 1.

UV-visible extinction spectra show that NOM improves the colloidal stability of citrate-capped AgNPs more significantly than PVP-capped AgNPs, and that the degree of colloidal stabilization conferred by NOM for both particle types was SRFA < SRHA << PLFA. Spectra of citrate-capped (top) and PVP-capped (bottom) AgNPs in pH 7.5 phosphate buffer were collected after incubation of AgNPs with NOM type specified. Shown are spectra measured at 1–6 (red), 11, 20, 24, 30, and 46 h (violet) after particle redispersion; arrows indicate directions of peak intensity changes. The peak near 390 nm corresponds to extinction by the primary (12-nm-diameter) particle population and peaks at longer wavelengths correspond to aggregates. Aggregate settling decreases peak intensities as it removes particles from the probed sample volume. The feature observed around 650 nm is an instrumental artifact. Results were duplicated in independent experiments.

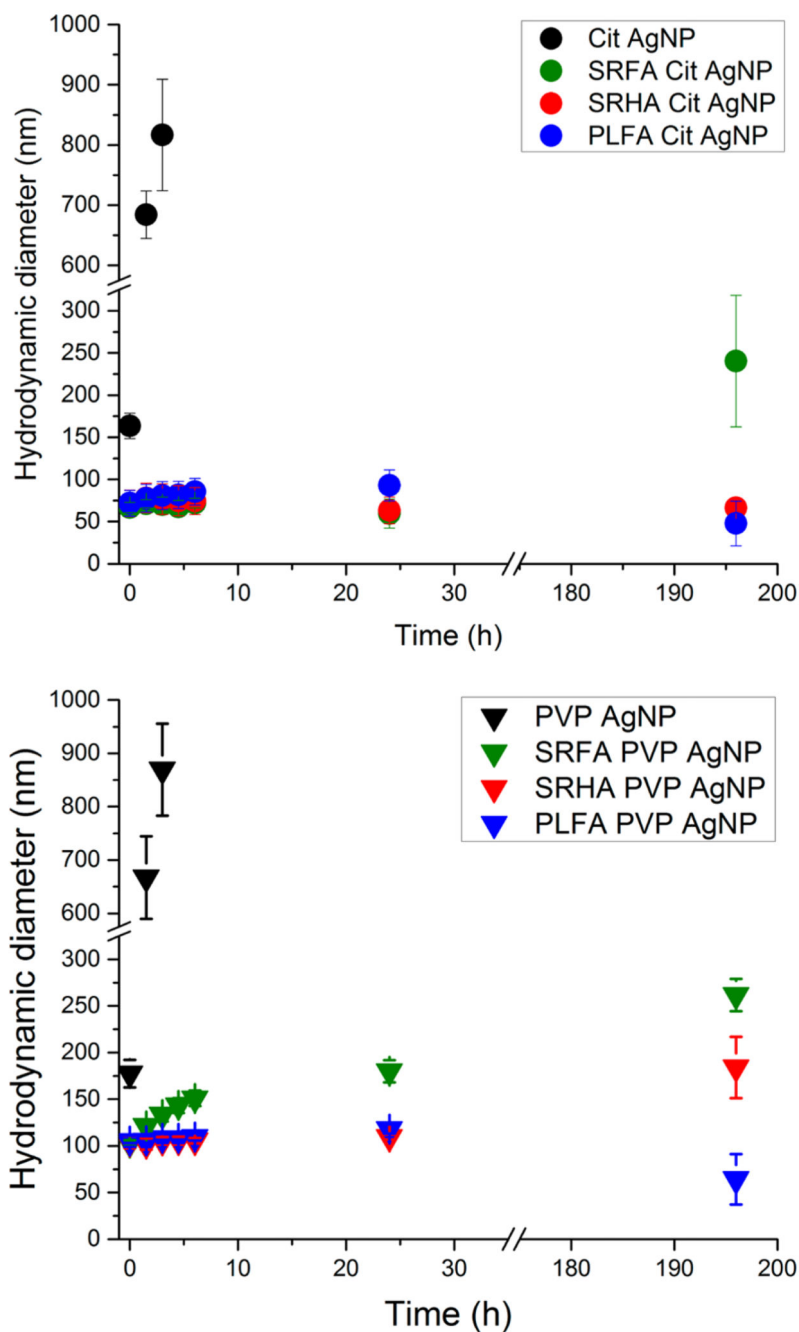
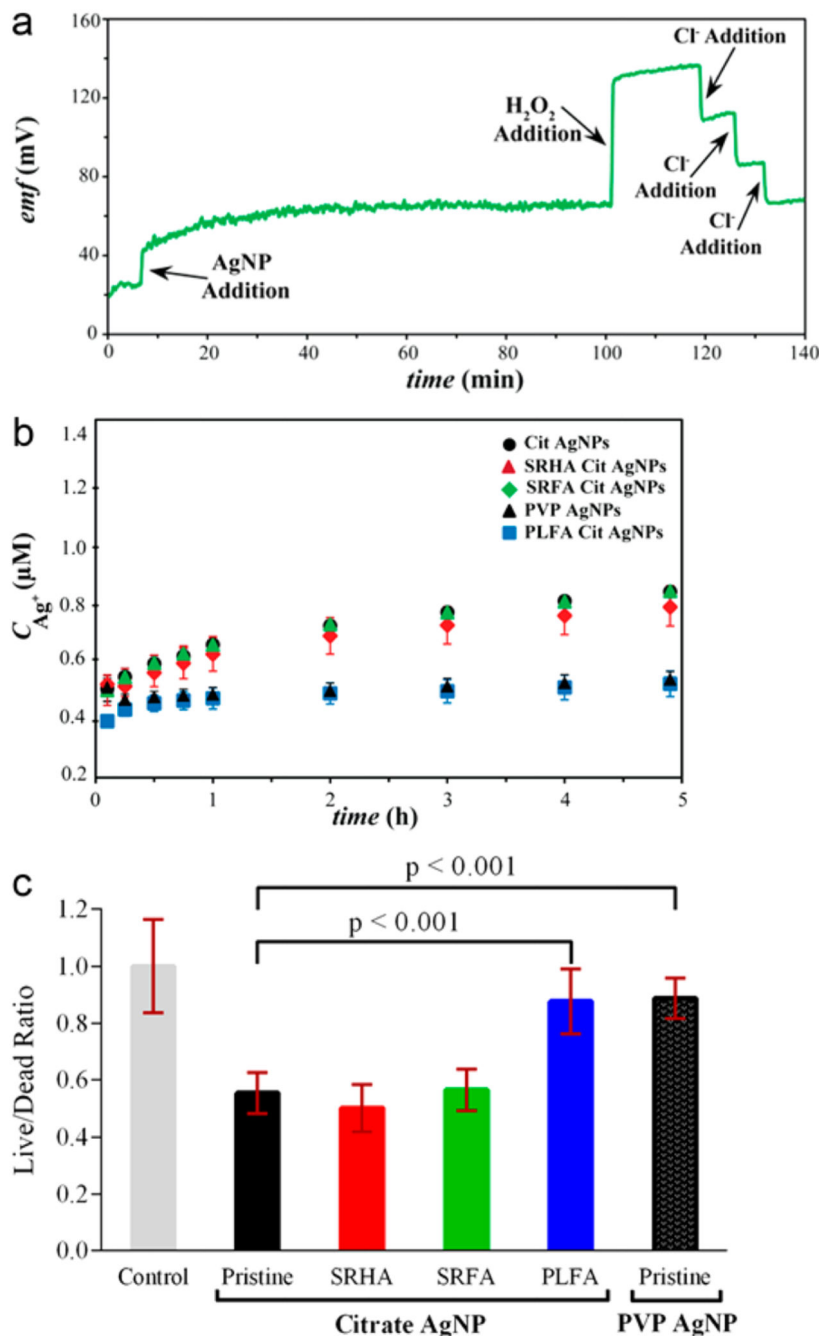


Figure 2. Average hydrodynamic diameters (Z-average particle size) of citrate-capped (top) and PVP-capped (bottom) AgNPs previously incubated with the NOM type specified after dispersion in buffer, as estimated with DLS. Error bars represent standard deviations of three independent replicates, each consisting of three analytical replicates.

**Figure 3.**

(a) Continuous detection with fluoros-phase Ag⁺ ISEs: 5 mg Ag/L citrate-capped AgNPs were added to pH = 7.5 buffer while monitoring the Ag⁺ release. H₂O₂ was added to oxidize AgNPs, and Cl⁻ was added to reduce the Ag⁺ concentration. (b) Dissolution of citrate-capped and PVP-capped AgNPs in pH 7.5 buffer (5 mg Ag/L) with or without prior incubation with NOM (nonsurface bound NOM concentration 10 mg/L). Error bars represent standard deviations of three replicate measurements. (c) Effect of AgNPs on *Shewanella* membrane integrity as a function of NOM type, as evaluated using fluorescent

dyes; shown is the ratio of fluorescence emission intensities for a membrane permeable dye (indicating live cells) and a membrane impermeable dye (indicating dead cells). Data collected from cells exposed to pristine nanoparticles (NP) and cells exposed to nanoparticles previously incubated with 600 mg/L NOM (PLFA-NP, SRFA-NP, and SRHA-NP) at the specified concentration were normalized to a negative control from *Shewanella* not exposed to nanoparticles; values smaller than 1 indicate decreased membrane integrity following nanoparticle exposure. Error bars represent standard deviations of three biological replicates.

Author Manuscript

Author Manuscript

Author Manuscript

Author Manuscript